Development and validation of a 3D CFD model of drift and its application to air assisted orchard sprayers

Ashenafi T. Duga[1], Mulugeta A. Delele[1], Kris Ruysen[3], Donald Dekeyser[2], David Nuyttens[2], Dany Bylemans[1,3], Bart M. Nicolai[1], Pieter Verboven[1]

[1]KU Leuven - University of Leuven, Department of Biosystems, MeBioS, De Croylaan 42, 3001 Leuven, Belgium

[2]Institute for Agricultural and Fisheries Research (ILVO) - Technology and Food Science Unit - Agricultural Engineering, Burg. Van Gansberghelaan 115, 9820 Merelbeke, Belgium

[3]Research Station for Fruit Growing (PCFruit), Department of Ecology, Fruittuinweg 1, 3800 Sint-Truiden, Belgium

E-mail of corresponding authors: ashenafitilahun.duga@biw.kuleuven.be and pieter.verboven@biw.kuleuven.be

ABSTRACT

Pesticides play an important role in providing high crop yields by minimizing risks associated with the occurrence of pests. Some of the sprayed product may, however, move beyond the intended target and result in drift. Modelling approaches help to understand spray drift using computer simulations. However, modelling drift from orchard spraying presents particular challenges: (1) the moving spray interacts with the canopy before reaching the drift area; (2) the vertical wind profile changes from the orchard to the neighbouring field that has a different vegetation; (3) the moving air jet from the air assistance cannot be ignored because the magnitude of the air jet velocity is typically higher than the wind velocity. As a result the modelling becomes rather complex.

This work presents a three-dimensional (3D) computational fluid dynamics (CFD) model of spray drift from orchard sprayers that considers the actual tree architecture, the canopy wind flow and the moving sprayer outlet to calculate sedimenting and airborne drift; thus tackling each of the above challenges. The CFD model was validated against drift measurements from an apple orchard with different nozzles arrangements. This model was then used to evaluate the effect of drift reducing nozzles and fan speed on drift. Drift reducing nozzles reduced the drifting distance by 50%, but increased near-tree ground deposition. The increase in ground deposition near the tree can be avoided (keeping the 50% reduction in the drifting distance) by combining the drift reducing nozzles with the standard ones. A reduced sprayer airflow resulted in further reduction of the percentage drift.

Keywords: drift reduction, nozzle, tree model, Lagrangian model, fan speed, plant protection product

1. Introduction

Agrochemical sprays play a pivotal role in enhancing the productivity and quality of crops by minimizing losses. However, their benefits are not without risks. A significant portion of the sprayed material moves beyond the intended target and poses environmental, economic and health risks. These associated risks have been the subject of discussion among the scientific community for over half a century. The first comprehensive report on the physical principles and measurements of drift was published by Akesson and Yates (1964). They reported on drift damages to non-target susceptible crops from aerial applications. Since then, the focus of drift research has broadened and now includes bystander and resident exposure (Butler Ellis, Lane, O'Sullivan, Miller, Glass, 2010), surface water contamination and protection of aquatic life (FOCUS, 2007; Lee et al., 2013)

According to the ISO standard (ISO 22866, 2005), spray drift is defined as the quantity of plant protection product that is carried out of the treated area by the action of air currents during the application process. The amount of pesticide drifted beyond the treated area depends on spray application technique (Duga et al., 2015a; van de Zande et al., 2008), physiochemical properties of the sprayed material (Dorr et al., 2013; Hilz & Vermeer, 2013), canopy architecture (Duga et al., 2015a) and meteorological conditions (Arvidsson, Bergström, Kreuger, 2011; Duga et al., 2015c; Duga et al., 2015b). Field tests (Nuyttens, De Schampheleire, Baetens, Sonck, 2007) and wind tunnel experiments (Nuyttens et al., 2009) are mostly used to understand the mechanisms that govern pesticide drift, characterize the effect of the different factors involved and assess drift potential (De Schampheleire, Baetens, Nuyttens, Spanoghe, 2008; Donkersley & Nuyttens, 2011; Salyani, Miller, Farooq, Sweeb, 2013). However, they both use sampling techniques and the data obtained are not time resolved, consider a limited number of points in the drift plume, are highly influenced by meteorological conditions and data collection is labour and time consuming (Gregorio et al., 2014). Light detection and ranging (LIDAR) techniques are also used to some extent to monitor the airborne spray drift from aerial and ground sprayers (Gregorio, Rocadenbosch, Sanz, Rosell-Polo, 2015; Miller, Saliyani, Hiscox, 2003; Stoughton, Miller, Yang, Ducharme, 1997). However, this technique is mostly used to study the movement and dispersion of the pesticide plumes qualitatively and it is only recently that some researchers attempted to quantify droplet concentration in spray clouds using lidar (Gregorio et al., 2014, 2015; Khot et al., 2011).

The high temporal and geographical variation of most of the factors that affect pesticide drift (crop characteristics, equipment design and setup, field size and slope, and number of treatments) even in the same country make it difficult to monitor drift using experiments alone. Properly validated modelling approaches allow a controlled parameter analysis of the spraying process, thus better understanding of the contribution of each parameter. Few models have been developed and validated in the past few decades to study drift from aerial and ground spray applications (Baetens et al., 2007, 2009; Egan, Bohnenblust, Goslee, Mortensen, & Tooker, 2014; Kruckeberg, Hanna, Steward, & Darr, 2012; Nsibande, Dabrowski, van der Walt, Venter, & Forbes, 2015; Teske et al., 2002; Teske, Thistle, & Ice, 2003). Some of these models are empirical models developed through curve fitting (Lazzaro, Otto, Zanin, 2008; Rautman et al., 2001). The applicability of these models is limited to the site and the conditions under which the data used to develop them were collected. They are also mostly developed for a single pollution target. Holterman and van de Zande (2008, 2010) developed a cascade drift model to predict the spatial and temporal distribution of pesticide drift into a network of interconnected water bodies. The model computes spray drift to multiple water bodies using a generic drift function developed by multiple linear regression of a large set of random scenarios obtained from the IDEFICS drift model (Holterman et al., 1997). The other group of models are called mechanistic models that are developed based on a set of physical equations describing a process (Baetens et al., 2007, 2009; Teske et al., 2002; Teske et al., 2003). As such, they are independent of site and the conditions under which the data used to develop them were collected. However, the applicability of mechanistic models is also limited by their complexity and high computational demand. The most advanced and widely used among these is the AGDISP® model developed by the USDA Forest Service. An additional model (AgDRIFT) was separately created (spawned from AGDISP®) under a Cooperative Research and Development Agreement between the Spray Drift Task Force and its partners, the US EPA and the USDA Forest Service. The AgDRIFT model itself consists of three application modules that may be used to estimate downwind deposition of spray drift from aerial, ground boom and orchard/vineyard air blast applications. However, the orchard/air blast module is based on empirical curve fits of data from a few orchard field trials which limits its applicability outside the experimental conditions of the data it is developed from. Hence, there is a need to develop models that could be applied irrespective of the particular spraying situation. A new integrated CFD model of orchard sprayers that incorporates the real tree architecture and a porous medium to represent the leaves and small branches was developed and validated using field experiments (Endalew et al., 2010b; Duga et al., 2015b). This model takes into account the actual tree architecture, the canopy wind profile and sprayer air flow and computes the droplet trajectory from a moving sprayer using the Lagrangian particle tracking model. While it was validated using on-target and ground deposition within a single row of an orchard (Duga et al., 2015b), it currently doesn't predict drift from orchard sprayers. The objective of this study was thus to develop and validate a CFD model to predict the sedimenting and air borne drift from orchard sprayers. The model calculation of sedimenting drift from an air assisted orchard sprayer in a typical apple orchard in Belgium was compared to field trials. This model was used to evaluate the effect of drift reducing nozzles and fan speed on spray drift.

2. Materials and Methods

In the following sections the model and field trials used for validation are explained. To better understand the specific application, this section starts with a description of the field experiment, including the sprayer and nozzles used and a description of the drift measurements in an apple orchard. For this application, the corresponding CFD model is then explained. If another sprayer type, nozzle or orchard system is considered, the CFD model can be easily adapted to these as explained by Duga et al. (2015).

2.1. Field experiment

2.1.1. *Sprayer design*

A cross-flow sprayer with PTO driven axial fans (DuoProp, BAB Bamps, Sint-Truiden, Belgium) (Figure 1) was used for both the field trial and model development. One-sided spraying (right side of the sprayer) was considered in the trial. The velocity distribution of the sprayer air-jet and the spray characteristics of the nozzles used were measured before the drift field trials and used as inputs for the CFD model. A hot wire anemometer (air velocity transducer, model 8465, TSI, Shoreview, MN, USA) was placed as close as possible to the sprayer outlet to measure the airflow. Additional measurements were performed using 3D ultrasonic sensors (model 81000, Young, Traverse City, MI, USA) placed at 0.15 m perpendicular to the outlet. The air flow measurements were taken at a horizontal interval of 0.05 m following the contour of the air outlet. Figure 1 shows the vertical profile of the measured 3D velocity components of the sprayer air-jet. Details of the air flow measurements are given in Dekeyser et al. (2013).

The total air flow rate estimated using the measured air velocities and the corresponding outlet area was 50,000 (m^3 h^{-1}) and 40,000 (m^3 h^{-1}) for the high and low fan speed settings respectively. A total of eight standard Albuz ATR orange and TVI 8002 drift reducing nozzles (Saint-Gobain Solcera, Évreux, France) were fitted to one side of the sprayer using the arrangements described in the next section. These nozzles were operating at a pressure of 600 kPa producing a spray with a volume median diameter of 155.8 µm and 380 µm, respectively. The sprayer was operated at an application rate of 500 (L ha^{-1}) and a driving speed of 1.67 (m s^{-1}) spraying only one side of the row.

2.1.2. *Nozzle arrangements*

Drift from three different nozzle arrangements was analysed using the cross-flow sprayer. The first arrangement was using the standard Albuz ATR orange hollow cone nozzles at all eight positions of the prayer which is represented here after by ATR (Figure 2a), the second arrangement was using Albuz TVI 8002 yellow drift reducing nozzles at all eight nozzle positions which is represented here after by TVI (Figure 2b) and the last arrangement was a combination of the two nozzles types (Albuz TVI 8002 yellow nozzles used at the top three positions and standard Albuz ATR orange hollow cone nozzles used at the bottom five positions) which is represented here after by (ATR+TVI) (Figure 2c).

The spray characteristics of the nozzles were measured using a one-dimensional Phase Doppler Particle Analyser system (PDPA, Aerometrics) (Nuyttens, Baetens, De Schampheleire, & Sonck, 2007). The measured particle size distributions of the different nozzles types were then fitted to a Rosin-Rammler distribution. However, the best Rosin-Rammler fit that was obtained for the Albuz TVI 8002 yellow drift reducing nozzles was not as good as for the standard Albuz ATR orange nozzles (Figure 2d). Hence, the measured size distributions were used in the model for both nozzles types. The Albuz TVI 8002 drift reducing nozzles used in this analysis have a 50% drift reduction according to the Belgian buffer zone regulation (Anon, 2004).

2.1.3. *Drift measurement*

The field experiments were conducted in an experimental orchard in October 2013 (pcfruit, Sint-Truiden, Belgium) containing three year old apple trees under classical training system. Trials were performed with the three nozzle arrangements discussed in the previous section on the cross flow sprayer. The trees in the orchard were arranged North-South with an interplant spacing of 1 m. The inter-row spacing was 3.2 m. Replicate measurements were done three lines from neighbouring trees in a row. The trees used for the field trial were 2.6 ± 0.3 m high and 1.4 ± 0.3 m wide. A measurement protocol that was prepared in accordance to the ISO standard (ISO 22866, 2005) was used to measure the sedimenting drift. However, single side spraying was used on the inner side of the last row, spraying outward, for the purpose of model validation. This spraying is considered to contribute the majority of drift downwind from the orchard but it should be realised that the measurements could not be considered a full drift trial. Sprayings were carried out in three repetitions for each nozzle configuration only on the last row of trees using metal tracers Cobalt, Manganese and Magnesium at an intended concentration of 4000 ppm.

After spraying, the samplers from each sampling position were collected and stored at 4 °C in dark conditions. The samplers were then washed with 0.16 N HNO_3 solution to extract the concentration of the tracer. The diluted solution in the test tubes was shaken for a minute and then the samplers were removed from the solution. The amount of metal tracer collected on each sampler was analysed using a Varian SpectrAA 300 atomic absorption spectrometer (AAS) (Varian Inc., CA, USA). The spray depositions at different distance and height were calculated using the surface area of the samplers. The sedimenting drift at a given distance were then calculated as a percentage of the total amount sprayed.

Campbell scientific weather station (Campbell Scientific, Utah, USA) was placed at 50 m from the sampling position to monitor wind velocity and temperature at three heights (1, 2 and 3 m), relative humidity at 2 m, and wind velocity and direction at 3.5 m. Wind speed and direction were measured at 10 m height using a 3D ultrasonic anemometer (Metek GmbH, Elmshorn, Germany), at 10 Hz. All measured meteorological data (wind velocity and direction, temperature, relative humidity) were used as inputs to the model.

2.2. CFD model

A CFD orchard drift model was developed based on an existing CFD model for predicting the on-target spray distribution in orchards (Duga et al., 2015b). The model considers the real architecture of the trees, the canopy wind flow (including both the within-canopy wind flow and the above-canopy wind flow up to 3 times the canopy height) and the moving sprayer outlet with dedicated spray nozzles. It then computes the tracks of representative droplets of the nozzle size distribution from the nozzle to the target, to non-target surfaces directly around the tree and the ones remaining in the air. This model was validated with on-tree measurements of deposition (Duga et al., 2015b). The model considered trees within the bulk of the orchard and was restricted to a small domain around a single tree and two neighbouring trees. For drift, however, a larger domain needs to be considered to predict the ground and airborne drift at larger distances behind a side row of trees. A computational domain having 40 m length and 50 m width was used in this work to represent the drift area next to the row of three orchard trees (Figure 4). The atmosphere was considered to 12 m high to include the lower part of the orchard boundary layer and the maximum sampling position used during the field trials. The 3D architecture of the trees was developed from the coordinate data collected during the field trials and used in the model simulations. Details on the development of the tree architecture can be found in Endalew et al. (2011). Only the outlet of the sprayer was represented in the model using a rectangular cross-section. The measured outlet velocity profile of the sprayer was applied to this cross-section to represent the right side of half of the sprayer.

The wind and the air flow from the sprayer were modelled using the unsteady Reynolds Averaged Navier-Stokes (URANS) equations and the k-ϵ turbulence model which were solved using the unstructured finite volume method in a CFD code of ANSYS-CFX (ANSYS, Inc., Canonsburg, Pennsylvania, USA). The airflow model computed the transient airflow pattern from the sprayer and its interaction with the wind and trees as the sprayer drives along the row. The effect of wind was integrated into the model using a canopy wind profile which was obtained from a series of steady RANS simulations over the computational domain to match the average measured wind velocity and direction of each trial obtained by the 3D anemometer at 10 m height above the canopy, according to the procedure explained by Endalew et al. (2009). A series of cyclic simulations were done using the measured wind speeds to determine a realistic canopy wind profile that was used in the model simulations. Each next simulation used the outlet profiles of the previous simulation as inlet boundary condition. The procedure was repeated until the difference between the inlet and outlet profiles of consecutive simulations became insignificant. A normalized root-mean-square (r.m.s) residual of less than 10^{-6} was used as the convergence criterion for the steady state simulations. The resulting canopy profiles were then imposed as input profiles at the boundaries of the domain depending on the wind direction. The URANS model was then solved by superimposing the outlet velocity profile of the sprayer which was defined as a moving boundary conditions at the driving speed of the orchard sprayer to the canopy wind profile. This transient airflow model used the steady canopy wind profile from the cyclic simulations as an initial condition. The turbulent boundary condition of the sprayer airflow was defined using a turbulent intensity of 30% and a length scale of 0.008 m (Delele et al., 2005). No-slip rough wall boundary conditions were used for the surfaces of the tree branches (equivalent sand grain roughness height (k_s) = 0.006 m) and the bottom boundary of the domain (roughness length (y_0) = 0.005 m) (Endalew et al., 2009). The other boundaries were set as atmospheric pressure openings to allow movement of air into and out of the domain. The resistance and turbulence effects of the leaves were modelled using closure models applied in the porous domain around the branches (Wilson & Shaw, 1977).

A Lagrangian particle tracking multiphase flow model was used to calculate the instantaneous position of the spray droplets in the turbulent airflow field around the trees and in the drift zone behind the trees (Delele et al., 2007). The model uses the measured nozzle and spray parameters (spray angle, liquid flow rate and pressure, nozzle size, droplet size distribution) to track the droplets. The accuracy of a Lagrangian particle tracking model highly depends on the number of particles injected (Graham & Moyeed, 2002). In this work, 3000 particles were injected per timestep based on the sensitivity study of Delele et al. (2007). The deposition of droplets on the leaves was modelled using a stochastic deposition model which is a function of the optical porosity of the trees (Endalew et al., 2010a). This model calculates the amount of droplets captured by the porous domain using the vertical profile of the optical porosity. The vertical profile of optical porosity was calculated from the leaf area density and width of the tree (Raupach, Woods, Dorr, Leys, Cleugh, 2001). The computational domain was discretized using an unstructured tetrahedral mesh combined with prismatic layers near the ground. The initial mesh size and the smallest mesh size near the surface of the tree branches were selected based on the required minimum dimensionless distance from the wall (y^+) for the turbulent wall functions to be valid (Kuzmin, Mierka, Turek, 2007). This resulted in a total of 11 839 661 elements and 2 184 962 nodes to simulate the cross-flow sprayer for the different settings. The calculations took a total CPU time of 83 hours using three computing nodes on a KU Leuven HPC Linux cluster each having 64 GB of RAM. The model was solved for the cross-flow sprayer in an apple orchard and validated using dedicated field trials. It was then used to compare spray drift from the three nozzle arrangements and two fan speeds. Simulations were done with the cross-flow sprayer using the droplet size distributions measured from the three nozzle setups. These simulations were done for the same wind condition of magnitude 3.0 (m s^{-1}) measured at 10 m height blowing in the direction of spraying. The model can easily be adapted to other sprayer types and training systems (Duga et al., 2015b).

The prediction error of the model was analysed using the Root-Mean-Squared-Error (RMSE). The RMSE was estimated using the relation RMSE = $\sqrt{\frac{1}{n}\sum_{i=1}^{n}(X_{e,i} - X_{m,i})^2}$ where $X_{e,i}$ is the measured value and $X_{m,i}$ is the model prediction at position *i*. The normalized RMSE values which were calculated using the range of the measurements (the maximum minus minimum values) were then used to assess the prediction accuracy of the model.

3. Results

3.1. Validation of the simulated drift curves

The drift curves were validated for three different nozzle arrangements (ATR, TVI, ATR+TVI) fitted to the cross-flow sprayer. A 3.0 to 3.9 (m s^{-1}) magnitude wind was blowing from north-east when the drift measurements were done using ATR nozzles (Figure 5a). The magnitude of the wind registered during the experiment with the TVI nozzles was relatively more variable and ranged from 1.0 to 4.6 (m s^{-1}) (Figure 5b). This wind was originally blowing from north-east and later shifted to an easterly wind. The wind registered during the experiment with the ATR+TVI nozzles had a magnitude ranging from 1.6 to 3.9 (m s^{-1}). This wind was also originally blowing from north-east and later changed direction to an easterly wind (Figure 5c).

Figures 6a-c show a comparison of the experimental measurements and model predictions for these three nozzle arrangements. The black and red lines in these plots represent the measured values and model predictions, respectively. As can be seen from the sedimenting drift qualitative plots in Figure 6, the model results are in a good agreement with the experimentally determined drift values. The model in general predicted the trend of the drift curves very well with some differences in the degree of agreement among the three nozzle arrangements. The model had a prediction error of 26%, 23% and 32% for the three nozzle arrangements: ATR, TVI and ATR+TVI, respectively. This prediction error is attributed to the temporal variations in wind conditions, the effect of branch movement and droplet evaporation which are not considered in the model. As can be seen from the wind rose plot in Figure 5, there was a difference in the dynamics of the wind even among the field trials for the three nozzle arrangements. The wind registered when the field trials were conducted using the TVI drift reducing nozzles and the ATR+TVI nozzles (Figure 5b and 5c) was relatively more variable both in magnitude and direction than the wind registered during the trial with the ATR nozzles (Figure 5a). However, the prediction error of the model for the field trial with ATR nozzles is higher than the one with TVI nozzles. This could be mainly because of the difference in the droplet size distribution generated by these two nozzle types as well as the factors given above. The Albuz ATR orange nozzles generated higher percentage of smaller sized droplets than the Albuz TVI yellow nozzles. These small droplets tended to stay much longer in the air and were more susceptible to dynamic wind effects than the mainly coarse droplets from the Albuz TVI nozzles which fell to the ground after a relatively shorter time in air. This shows that droplet size distribution also plays a significant part in the complex interplay between spray, canopy and meteorological parameters to decide the final fate of spray droplet and the extent of drift from orchard sprayers.

3.2. Effect of nozzle arrangement on drift

Figure 7 presents the droplet track plots coloured according to the droplet size for the three nozzle arrangements. This plot shows the transient position of the droplets up to 40 m behind the last row of trees. Figure 7a shows the droplet track plot obtained when ATR nozzles were used on the cross-flow sprayer. As can be seen from this plot, most of the spray droplets are still airborne even after 40 m behind the tree row. This can be explained by the droplet size distribution generated by the Albuz ATR orange nozzles. These nozzles are characterized by a high percentage of fine droplets as shown in Figure 2. The maximum droplet size obtained from standard Albuz ATR orange nozzles is 430 µm. These fine droplets remain suspended in air for a longer time and cause drift at larger distances.

The droplet track plots obtained when TVI nozzles were used at all eight positions on the cross-flow sprayer is shown in Figure 7b. It can be seen from this plot that a significant portion of the droplets have already fallen to the ground in the first 20 meters. There are relatively fewer droplets that are still airborne than when ATR nozzles were used. The mainly coarse droplets from this nozzle fall to the ground much quicker than the droplets from the standard Albuz ATR orange nozzles. 45 % of the spray droplets generated by the Albuz TVI 8002 drift reducing nozzles have a diameter greater than the maximum droplet size generated by the standard Albuz ATR orange nozzles (Figure 2). Previously, indoor trials and CFD simulations were performed using these three nozzle arrangements on the cross-flow sprayer to study the spray distribution around the tree (Duga et al., 2014). When the Albuz TVI 8002 drift reducing nozzles were used, a relatively higher proportion of droplets deposited on the ground before reaching the canopy than when the standard Albuz ATR orange nozzles were used. This could compromise the on-target deposition depending on the wind and canopy density. However, it has been shown for the configurations considered in this study that the two nozzle types could be used together to limit their individual disadvantages and combine the best of both worlds.

Figure 7c presents the droplet track plot obtained when ATR+TVI nozzle are used. This plot shows that the droplet trajectory obtained for this set-up is an intermediate between the two nozzle types with relatively lower proportion of droplets still airborne than the standard Albuz ATR orange nozzles.

Figure 8 shows contour plots of the time integrated spray deposition on the ground at different horizontal distances behind the tree row for the three nozzle arrangements obtained from the CFD simulation. As can be seen from this figure, ATR nozzles gave a ground deposition up to 40 m behind the trees (Figure 8a). This ground deposition reduced to only 20 m when TVI drift reducing nozzles are used (Figure 8b). The TVI drift reducing nozzles reduced the drifting distance by half. However, these nozzles resulted in a higher deposition closer to the tree. The ATR+TVI combination gave a relatively lower ground deposition closer to the tree than the TVI nozzles but drift was detected at a farther distance (Figure 8c). It can also be seen from this figure that there is an apparent deviation of the spray path around the trees. This is due to the small number of trees considered (three trees in a row) in the model. This also contributed to the deviation between the measurement and model prediction in the first few meters behind the trees as shown in Figure 6. This could be avoided in future investigations by considering more trees on either side of the row.

Figure 9 quantitatively summarizes the sedimenting drift up to a distance of 40 m behind the trees for the three nozzle arrangements. The TVI nozzles gave the highest percentage drift in the first 3 m behind the trees. From 3 m to 12 m, the TVI and ATR+TVI setups gave similar percentage drift which is larger than the percentage drift from the standard Albuz ATR orange nozzles. From 12 m to 40 m, the standard ATR nozzles gave the highest percentage drift. The sedimenting drift from the TVI nozzles and the ATR+TVI combination dropped to less than 1% in the first 20 m. The ATR nozzles maintained a percentage drift of close to 2% up to 40 m behind the trees. One should pay attention to the difference in the percentage drift among the different nozzle arrangements rather than the individual percentage drift values obtained for this particular situation. This analysis is done for fully-leafed trees which gave a maximum sedimenting drift of 20%. However, the sedimenting drift obtained from spraying a leafless trees could reach up to 40% (not reported). If the drift curves of the different setups are integrated from before the last tree to the 40 m point, then the ATR+TVI and TVI setups result in the same total amount of drift deposit, while the ATR setup has lower total deposition drift (approximately 16% less). This illustrates a complete analysis of the spray patterns is necessary to correctly interpret results.

3.3. Effect of fan speed on drift from three nozzle arrangements

The volumetric flow rate and velocity of air assistance is an important parameter that strongly influences drift from air assisted orchard sprayers. It transports the spray droplets to the target and moves the branches and leaves to allow better coverage and penetration. However, depending on the type of the canopy and the air flow, the spray could drop before reaching the tree or be carried further behind the trees causing environmental and health risks. Unfortunately, the cross-flow sprayer used in this study and many other commercial sprayers have little means to adjust the velocity and flow rate of air to a specific canopy. In this section, the effect of two fan speeds (low and high fan speed) on drift from three different nozzle arrangements fitted to a cross flow sprayer was analysed. The sprayer produced an airflow rate of 40,000 and 50,000 $m^3 h^{-1}$ operating at low and high fan speeds, respectively (Dekeyser et al., 2013). This indicates that increasing fan speed does not necessarily lead to drastic increases in volume airflow rates depending on the fan characteristics.

Figure 10 compares the sedimenting drift from three different nozzle arrangements fitted to the cross–flow sprayer operating at high and low fan speeds. The solid and broken lines in this plot represent the percentage drift at high and low fan speeds, respectively. As can be seen from figures 10a, 10b and 10c, the reduction in fan speed in general slightly increased the sedimenting drift close to the trees and decreased the drift values further behind the tree. This is expected as the reduction in fan speed decreases the strength of the air assistance to the spray droplets causing a portion of the spray that was supposed to travel behind the tree deposit nearby. However, the reduction in the drifting distance was not significant to the specific canopy and wind condition considered in this study. The effect of a reduction in fan speed is significant when there is a strong cross flow wind blowing perpendicular to the spraying direction (Cross, Walklate, Murray, Richardson, 2003) or when the canopy is very dense. The extent of drift reduction would be much more significant when the spraying is done on very dense canopy or in the presence of strong cross flow winds blowing perpendicular to the spraying direction.

4. Discussions

In general, further drift reduction than that which could be obtained using drift reducing nozzles can be achieved by operating the fans at low speed as previously reported by other researchers (Balsari et al., 2014; Landers, 2011). This was also seen in the results presented above although the difference was not significant for the specific spraying conditions considered. It has also been shown that the amount of droplets which drop to the ground close to the trees when operating at low fan speed could be decreased by using a combination of the standard Albuz ATR orange nozzles and Albuz TVI 8002 yellow drift reducing nozzles rather than using only Albuz TVI 8002 drift reducing nozzles. Care should however be taken when there is a strong cross flow wind blowing perpendicular to the spraying direction which makes the spray droplets highly susceptible to drift.

Droplet size distribution plays a very important role in deciding both the quality of treatment and amount of pesticide drift from air assisted orchard sprayers. The presence of a large proportion of fine droplets in the droplet size spectra increases the spray coverage at the expense of high drift. A large proportion of coarse droplets on the other hand reduces spray drift but results in poor coverage due to the tendency of coarse droplets to rebound from the leaf surface. It is possible to reduce spray drift from orchard sprayers without compromising the biological efficacy if it is possible to generate coarse droplets that have lower tendency to rebound. As suggested by previous researchers, this can be achieved by using either adjuvants (Miller, Hewitt, Bagle, 2001; Oliveira, Antuniassi, Mota, Chechetto, 2013; Salyani & Cromwell, 1993; Spanoghe, De Schampheleire, van der Meeren, Steurbaut, 2007) or air-induction (drift reducing) nozzles (Behmer, Di Prinzio, Striebeck, Magdalena, 2010; Derksen, Fox, Brazee, Krause, 2007; Mcartney & Obermiller, 2008; Wenneker, Heijne, van de Zande, 2005; Wenneker & van de Zande, 2008; Zhu, Guler, Derksen, Ozkan, 2005). However, some researchers reported no pronounced effect of adjuvants on droplet size (Fritz, Hoffmann, Bagley, 2012) and similar drift profiles by all conventional adjuvants (Butler Ellis & Tuck, 1999). The use of drift reducing nozzles to reduce spray drift by generating coarse droplets attracted the attention of many researchers due to the ballistic behaviour of the droplets. The air-filled droplets produced by these nozzles disintegrate into smaller droplets when they hit a solid surface and spread onto the target rather than bounce. Comparison of drift from drift reducing and conventional hydraulic nozzles by some researchers (Behmer et al., 2010; Wenneker et al., 2005; Zhu et al., 2005) showed a reduction in drift by drift reducing nozzles which is in line with the results obtained from this CFD analysis. Some researchers also reported that drift reducing nozzles give higher ground deposition near the orchard boundaries (Heijne, Wenneker, Van de Zande, Western, 2002; Wenneker et al., 2005; Wenneker & van de Zande, 2008; Zhu et al., 2005) which again conforms with the results of the CFD simulations performed in this study.

Several countries have developed their own guidelines and mitigation measures to reduce pesticides drift and most of them included the use of drift reducing nozzles as one. The Belgian Federal Public Service for Health, Food Chain Safety and Environment which is responsible for registering (licensing) pesticides for sale and use in Belgium has imposed eight drift mitigation requirements on pesticide product labels (Anon, 2004). The buffer zone requirement in this mitigation measures can be reduced using drift reducing nozzles. However, drift reducing nozzles should be used in combination with other techniques to avoid the high ground deposition near the orchard boundary which impairs the reduction in drift. Wenneker and van de Zande (2008) reported on the use of shielded sprayer to overcome the problem of high deposition near the orchard boundaries by these nozzles. In this work, the combined use of Albuz TVI drift reducing and Albuz ATR standard nozzles (top three drift reducing and bottom five Albuz ATR nozzles) on a cross-flow sprayer as a way to reduce the high ground deposition near the orchard boundaries was explored. It was interesting to see that it is possible to reduce the near orchard ground deposition while maintaining the same drift reduction as the drift reducing nozzles. In this work, simulations were performed for only one combination of nozzles and one sprayer type. It would be interesting to investigate other combinations of these two nozzle types and also other sprayer designs. The results reported in this work also showed that it is possible to reduce drift further by using the drift reducing nozzles on the cross-flow sprayer at low fan speed. The high ground deposition near the orchard boundary while operating the sprayer at low fan speed can be decreased by using a combination of drift reducing and standard Albuz ATR orange nozzles.

5. Conclusions

A CFD drift model of air assisted orchard spraying was successfully validated. This model was then used to study the effect of nozzle arrangement and fan speed on drift. One common downside of using drift reducing nozzles as a drift mitigation strategy is the high ground deposition observed near the orchard boundaries. This is especially important in areas where orchards are present near surface waters. This work investigated the potential of combining drift reducing and standard Albuz ATR nozzles as one drift mitigation strategy using CFD. The results of the study showed the potential of CFD modelling as a tool to investigate drift mitigation strategies. The analysis done using one combination of the two nozzle types showed that combining the standard Albuz ATR and drift reducing nozzles decreased the spray deposition close to the trees while achieving

50% reduction in drift distance. The combined use of these two nozzle types requires no complex sprayer design modification, which makes it easier and cheaper to implement. The presence of the standard nozzles that the farmers are familiar with may also avoid scepticism and make it easier to convince them.

The effect of high and low fan speeds on the percentage drift from three nozzle arrangements was further analysed using the CFD model. The results obtained showed that fan speed does not have a significant effect on drift for the spray conditions considered in this study. The developed model can be used to do further analysis on other mitigation strategies (more nozzle combinations and other sprayer designs). It can also be used to investigate the effect of other parameters (e.g. different wind magnitudes and directions) on drift from air assisted orchard sprayers.

Finally, the presented model overcomes the following challenges of orchard drift modelling in a physically resolved way:

(1) the moving spray interacts with the canopy before reaching the drift area: by modelling the tree architecture and leaf cover, the wind velocity changes across the tree row and droplets are captured and deviated before reaching the drift zone.

(2) the vertical wind profile changes from the orchard to the neighbouring field that has a different vegetation: the airflow field is solved by means of the governing equations continuously across the trees into and over the drift zone. From a canopy profile inside the orchard, the flow develops into an atmospheric boundary profile across the neighbouring drift field with a specified roughness height of the grass field. Flow paths around the specific tree training system are resolved and affect the drift profile.

(3) the moving air jet from the air assistance cannot be ignored because the magnitude of the air jet velocity is typically higher than the wind velocity: a dynamic model is implemented that resolves the moving sprayer outlet of the orchard sprayer over the tree row.

Acknowledgement

The financial support of the Institute for the Promotion of Innovation by Science and Technology in Flanders (project IWT 080528) is gratefully appreciated.

References

Akesson, B. N. B., & Yates, W. E. (1964). Problems relating to application of agricultural chemicals and resulting drift residues. Annual Review of Entomology, 9, 285–318.

Anon, 2004. Maatregelen ter beperking van de verontreiniging van oppervlaktewater door gewasbeschermingsmiddelen. Federal Public Service of Public Health, Food Chain Security and Environment, DG Animals, Plants & Food, Service Pesticides and Fertilizers. Brussels. P. 12.〈http://www.fytoweb.fgov.be/NL/doc/driftreducerende%20maatregelen%20voor%20gewasbeschermingsmiddelen.pdf〉

Arvidsson, T., Bergström, L., & Kreuger, J. (2011). Spray drift as influenced by meteorological and technical factors. Pest Management Science, 67(5), 586–598. doi:10.1002/ps.2114

Baetens, K., Ho, Q. T., Nuyttens, D., De Schampheleire, M., Endalew, A. M., Hertog, M. L. A. T. M., Nicolai, B., Ramon, H., Verboven, P. (2009). A validated 2-D diffusion-advection model for prediction of drift from ground boom sprayers. Atmospheric Environment, 43(9), 1674–1682. doi:10.1016/j.atmosenv.2008.12.047

Baetens, K., Nuyttens, D., Verboven, P., De Schampheleire, M., Nicolaï, B., & Ramon, H. (2007). Predicting drift from field spraying by means of a 3D computational fluid dynamics model. Computers and Electronics in Agriculture, 56(2), 161–173.

Balsari, P., Gil, E., Marucco, P., Gallart, M., Bozzer, C., Llop, J., & Tamagnone, M. (2014). Study and development of a test methodology to assess potential drift generated by air-assisted sprayers. Aspects of Applied Biology, 122, 339–346.

Behmer, S., Di Prinzio, A., Striebeck, G., & Magdalena, J. (2010). Evaluation of Low-Drift Nozzles in Agrochemical Applications in Orchards. Chilean Journal of Agricultural Research, 70(3), 498–502. doi:10.4067/S0718-58392010000300017

Butler Ellis, M. C., Lane, a. G., O'Sullivan, C. M., Miller, P. C. H., & Glass, C. R. (2010). Bystander exposure to pesticide spray drift: New data for model development and validation. Biosystems Engineering, 107(3), 162–168. doi:10.1016/j.biosystemseng.2010.05.017

Butler Ellis, M. C., & Tuck, C. R. (1999). How adjuvants influence spray formation with different hydraulic nozzles. Crop Protection, 18(2), 101–109. doi:10.1016/S0261-2194(98)00097-0

Cross, J. V., Walklate, P. J., Murray, R. A., & Richardson, G. M. (2003). Spray deposits and losses in different sized apple trees from an axial fan orchard sprayer: 3. Effects of air volumetric flow rate. Crop Protection, 22(2), 381–394. doi:10.1016/S0261-2194(02)00192-8

De Schampheleire, M., Baetens, K., Nuyttens, D., & Spanoghe, P. (2008). Spray drift measurements to evaluate the Belgian drift mitigation measures in field crops. Crop Protection, 27(3-5), 577–589. doi:10.1016/j.cropro.2007.08.017

Dekeyser, D., Duga, A. T., Verboven, P., Endalew, A. M., Hendrickx, N., & Nuyttens, D. (2013). Assessment of orchard sprayers using laboratory experiments and computational fluid dynamics modelling. Biosystems Engineering, 114(2), 157–169. doi:10.1016/j.biosystemseng.2012.11.013

Delele, M. A., De Moor, A., Sonck, B., Ramon, H., Nicolaï, B. M., & Verboven, P. (2005). Modelling and Validation of the Air Flow generated by a Cross Flow Air Sprayer as affected by Travel Speed and Fan Speed. Biosystems Engineering, 92(2), 165–174.

Delele, M. A., Jaeken, P., Debaer, C., Baetens, K., Endalew, A. M., Ramon, H., Nicolai, B.M., Verboven, P. (2007). CFD prototyping of an air-assisted orchard sprayer aimed at drift reduction. Computers and Electronics in Agriculture, 55(1), 16–27.

Derksen, R. C., Fox, R. D., Brazee, R. D., & Krause, C. R. (2007). Coverage and drift produced by air induction and conventional hydraulic nozzles used for orchard applications. In Transactions of the ASABE (pp. 1497–1501). American Society of Agricultural Engineers. doi:10.13031/2013.23941

Donkersley, P., & Nuyttens, D. (2011). A meta-analysis of spray drift sampling. Crop Protection, 30(7), 931–936. doi:10.1016/j.cropro.2011.03.020

Dorr, G. J., Hewitt, A. J., Adkins, S. W., Hanan, J., Zhang, H., & Noller, B. (2013). A comparison of initial spray characteristics produced by agricultural nozzles. Crop Protection, 53, 109–117. doi:10.1016/j.cropro.2013.06.017

Duga, A. T., Defraeye, T., Nicolai, B., Dekeyser, D., Nuyttens, D., Bylemans, D., & Verboven, P. (2014). Training system dependent optimization of air assistance and nozzle type for orchard spraying by CFD modelling. Aspects of Applied Biology, 122, 453–458.

Duga, A. T., Dekeyser, D., Ruysen, K., Bylemans, D., Nuyttens, D., Nicolai, B. M., & Verboven, P. (2015a). Numerical Analysis of the Effects of Wind and Sprayer Type on Spray Distribution in

Different Orchard Training Systems. Boundary-Layer Meteorology, 157(3), 1–19. doi:10.1007/s10546-015-0064-2

Duga, A., Ruysen, K., Dekeyser, D., Nuyttens, D., Bylemans, D., Nicolaï, B., & Verboven, P. (2015b). CFD Based Analysis of the Effect of Wind in Orchard Spraying. Chemical Engineering Transactions, 44, 1–6.

Duga, A. T., Ruysen, K., Dekeyser, D., Nuyttens, D., Bylemans, D., Nicolai, B. M., & Verboven, P. (2015c). Spray deposition profiles in pome fruit trees: Effects of sprayer design, training system and tree canopy characteristics. Crop Protection, 67, 200–213. doi:10.1016/j.cropro.2014.10.016

Egan, J. F., Bohnenblust, E., Goslee, S., Mortensen, D., & Tooker, J. (2014). Herbicide drift can affect plant and arthropod communities. Agriculture, Ecosystems & Environment, 185, 77–87. doi:10.1016/j.agee.2013.12.017

Endalew, A. M., Debaer, C., Rutten, N., Vercammen, J., Delele, M. A., Ramon, H., Nicolaï, B. M., Verboven, P. (2010a). A new integrated CFD modelling approach towards air-assisted orchard spraying. Part I. Model development and effect of wind speed and direction on sprayer airflow. Computers and Electronics in Agriculture, 71(2), 128–136. doi:10.1016/j.compag.2009.11.005.

Endalew, A. M., Debaer, C., Rutten, N., Vercammen, J., Delele, M. A., Ramon, H., Nicolaï, B. M. Verboven, P. (2010b). Modelling pesticide flow and deposition from air-assisted orchard spraying in orchards: A new integrated CFD approach. Agricultural and Forest Meteorology, 150(10), 1383–1392. doi:10.1016/j.agrformet.2010.07.001

Endalew, A. M., Debaer, C., Rutten, N., Vercammen, J., Delele, M. A., Ramon, H., Nicolaï, B. M., Verboven, P. (2011). Modeling the Effect of Tree Foliage on Sprayer Airflow in Orchards. Boundary-Layer Meteorology,138, 139–162. doi: 10.1007/s10546-010-9544-6

Endalew, A. M., Hertog, M., Gebrehiwot, M. G., Baelmans, M., Ramon, H., Nicolaï, B. M., & Verboven, P. (2009). Modelling airflow within model plant canopies using an integrated approach. Computers and Electronics in Agriculture, 66(1), 9–24.

FOCUS. (2007). Landscape and mitigation factor Report of the FOCUS Working Group on Landscape and Mitigation Factors in Ecological Risk Assessment. EC Document Reference SANCO/10422/2005 V.2.0, Aquatic Risk Assessment. Extended Summary and Recommendations.

Fritz, B. K., Hoffmann, W. C., & Bagley, W. E. (2012). Effects of Formulated Glyphosate and Adjuvant Tank Mixes on Atomization from Aerial Application Flat Fan Nozzles. Pesticide Formulation and Delivery Systems: Innovating Legacy Products for New Uses, 32, 80–95. doi:10.1520/STP104451

Graham, D. I., & Moyeed, R. a. (2002). How many particles for my Lagrangian simulations? Powder Technology, 125(2-3), 179–186. doi:10.1016/S0032-5910(01)00504-6

Gregorio, E., Rocadenbosch, F., Sanz, R., & Rosell-Polo, J. (2015). Eye-Safe Lidar System for Pesticide Spray Drift Measurement. Sensors, 15(2), 3650–3670. doi:10.3390/s150203650

Gregorio, E., Rosell-Polo, J. R., Sanz, R., Rocadenbosch, F., Solanelles, F., Garcerá, C., Chueca, P., Arnó, J., del Moral, I., Msip, J., Camp, F., Viana, R., Escola, A., Garcia, F., Planas, S.,Moltó, E. (2014). LIDAR as an alternative to passive collectors to measure pesticide spray drift. Atmospheric Environment, 82, 83–93. doi:10.1016/j.atmosenv.2013.09.028

Heijne, B., Wenneker, M., Van de Zande, J. C., & Western, N. M. (2002). Air inclusion nozzles don't reduce pollution of surface water during orchard spraying in the Netherlands. In Aspects of Applied Biology (pp. 193–199).

Hilz, E., & Vermeer, A. W. P. (2013). Spray drift review: The extent to which a formulation can contribute to spray drift reduction. Crop Protection, 44, 75–83. doi:10.1016/j.cropro.2012.10.020

Holterman, H., Van de Zande, J., Porskamp, H. a J., & Huijsmans, J. (1997). Modelling spray drift from boom sprayers. Computers and Electronics in Agriculture, 19(1), 1–22. doi:10.1016/S0168-1699(97)00018-5

Holterman, H., & Van de Zande, J.. (2008). The Cascade Drift Module : a GIS-based study on regional pesticide deposition. In Aspects of Applied Biology (Vol. 84, pp. 83–90).

ISO 22866. 2005. International Standard: Crop protection equipment - Methods for field measurement of spray drift. (2005).

Khot, L. R., Miller, D. R., Hiscox, A. L., Salyani, M., Walker, T. W., & Farooq, M. (2011). Extrapolation of Droplet Catch Measurements in Aerosol Application Treatments. Atomization and Sprays, 21(2), 149–158. doi:10.1615/AtomizSpr.2011002846

Kruckeberg, J. P., Hanna, H. M., Steward, B. L., & Darr, M. J. (2012). The Relative Accuracy of DRIFTSIM When Used as a Real-Time Spray Drift Predictor. Transactions of the ASABE, 55(4), 1159–1165.

Kuzmin, D., Mierka, O., & Turek, S. (2007). On the implementation of the κ-ε turbulence model in incompressible flow solvers based on a finite element discretisation. International Journal of Computing Science and Mathematics, 1(2/3/4), 193. doi:10.1504/IJCSM.2007.016531

Landers, A. (2011). Improving Spray Deposition with Engineering Innovation - What a Difference a Decade Makes. Research Focus, pp. 1–7.

Lazzaro, L., Otto, S., & Zanin, G. (2008). Role of hedgerows in intercepting spray drift: Evaluation and modelling of the effects. Agriculture, Ecosystems & Environment, 123(4), 317–327. doi:10.1016/j.agee.2007.07.009

Lee, I. B., Bitog, J. P. P., Hong, S. W., Seo, I. H., Kwon, K. S., Bartzanas, T., & Kacira, M. (2013). The past, present and future of CFD for agro-environmental applications. Computers and Electronics in Agriculture, 93, 168–183. doi:10.1016/j.compag.2012.09.006

Mcartney, S. J., & Obermiller, J. D. (2008). Comparative Performance of Air-induction and Conventional Nozzles on an Axial Fan Sprayer in Medium Density Apple Orchards. HortTechnology, 18(3), 365–371.

Miller, D. R., Saliyani, M., & Hiscox, A. B. (2003). Remote Measurement of Spray Drift from Orchard Sprayers Using LIDAR. In Transactions of the ASABE (p. Paper number 031093).

Miller, P. C. H., Hewitt, A. J., & Bagle, W. E. (2001). Adjuvant effects on spray characteristics and drift potential. ASTM STP 1414: Pestesticide Formulations and Application Systems, 21, 175–184.

Nsibande, S. a., Dabrowski, J. M., van der Walt, E., Venter, A., & Forbes, P. B. C. (2015). Validation of the AGDISP model for predicting airborne atrazine spray drift: A South African ground application case study. Chemosphere, 138, 454–461.

Nuyttens, D., Baetens, K., De Schampheleire, M., & Sonck, B. (2007a). Effect of nozzle type, size and pressure on spray droplet characteristics. Biosystems Engineering, 97, 333–345. doi:10.1016/j.biosystemseng.2007.03.001

Nuyttens, D., De Schampheleire, M., Baetens, K. & Sonck., B. (2007b). The Influence of Operator-Controlled Variables on Spray Drift from Field Crop Sprayers. Transactions of the ASABE, 50(4), 1129–1140. doi:10.13031/2013.23622

Nuyttens, D., Taylor, W. A., De Schampheleire, M., Verboven, P., & Dekeyser, D. (2009). Influence of nozzle type and size on drift potential by means of different wind tunnel evaluation methods. Biosystems Engineering, 103(3), 271–280. doi:10.1016/j.biosystemseng.2009.04.001

Oliveira, R. B. De, Antuniassi, U. R., Mota, A. a. B., & Chechetto, R. G. (2013). Potential of adjuvants to reduce drift in agricultural spraying. Engenharia Agrícola, 33(5), 986–992. doi:10.1590/S0100-69162013000500010

Raupach, M. R., Woods, N., Dorr, G., Leys, J. F., & Cleugh, H. a. (2001). The entrapment of particles by windbreaks. Atmospheric Environment, 35(20), 3373–3383. doi:10.1016/S1352-2310(01)00139-X

Rautmann D, Streloke M, W. R. (2001). New basic drift values in the authorization procedure for plant protection products. Mitt. Biol.Bundesanst. Land Fiorst-Wirtsch, 383, 133–141.

Salyani, M., & Cromwell, R. P. (1993). Adjuvants to reduce drift from handgun spray application. ASTM STP 1146:Pesticide Formulations and Application Systems, 12, 363–376.

Salyani, M., Miller, D. R., Farooq, M., & Sweeb, R. D. (2013). Effects of sprayer operating parameters on airborne drift from citrus air-carrier sprayers. Agric Eng Int: CIGR Journal, 15(1), 27–36.

Spanoghe, P., Schampheleire, M. De, & Meeren, P. Van Der. (2007). Influence of agricultural adjuvants on droplet spectra. Pest Management, 63, 4–16. doi:10.1002/ps

Stoughton, T. E., Miller, D. R., Yang, X., & Ducharme, K. M. (1997). A comparison of spray drift predictions to lidar data. Agricultural and Forest Meteorology, 88(1-4), 15–26. doi:10.1016/S0168-1923(97)00056-7

Teske, M. E., Bird, S. L., Esterly, D. M., Curbishley, T. B., Ray, S. L., & Perry, S. G. (2002). AgDRIFT: a model for estimating near-field spray drift from aerial applications. Environmental Toxicology and Chemistry / SETAC, 21(3), 659–671. doi:10.1002/etc.5620210327

Teske, M. E., Thistle, H. W., & Ice, G. G. (2003). Technical advances in modelling aerially applied sprays. Transactions of the ASAE, 46(4), 985–996.

Van De Zande, J. C., Huijsmans, J. F. M., Porskamp, H. a J., Michielsen, J. M. G. P., Stallinga, H., Holterman, H. J., & De Jong, a. (2008). Spray techniques: How to optimise spray deposition and minimise spray drift. Environmentalist, 28(1), 9–17. doi:10.1007/s10669-007-9036-5

Wenneker, M., Heijne, B., & Van de Zande, J. C. (2005). Effect of air induction nozzle (coarse droplet), air assistance and one-sided spraying of the outer tree row on spray drift in orchard spraying. Annual Review of Agricultural Engineering, 4(1), 116–128.

Wenneker, M., & Van de Zande, J. (2008). Drift Reduction in Orchard Spraying Using a Cross Flow Sprayer Equipped with Reflection Shields (Wanner) and Air Injection Nozzles. Agricultural Engineering International: The CIGR Ejournal. Manuscript ALNARP, 8, 014.

Wilson, N. R., & Shaw, R. H. (1977). A higher order closure model for canopy flow.pdf. Journal of Applied Meteorology, 16, 1197–1205.

Zhu, H., Guler, H., Derksen, R. C., & Ozkan, H. E. (2005). Comparison of Airborne and Ground Spray Deposits with Hollow Cone Nozzle , Low Drift Nozzle and Drift Retardant. In 9th International Congress on Mechanization and Energy in Agriculture & 27th International Conference of CIGR Section IV: The Efficient Use of Electricity and Renewable Energy Sources in Agriculture (pp. 27–29). Izmir-Turkey.

Figure captions

Figure 1 The three components of the outlet velocity of the Cross-flow sprayer (Duoprop, BAB-Bamps, Sint-Truiden, Belgium) used in the analysis operating at high (a) and low fan speeds (b): U (, horizontal perpendicular to driving direction), V (, vertical upward) and W (, horizontal in the driving direction). The outlet velocities were measured at 0.15 m from the outlet area at different heights using 3D ultrasonic sensors (Dekeyser et al., 2013).

Figure 2 The droplet size distributions and the corresponding Rossin-Rammler fits of the two nozzle types. The broken lines represent the measured size distributions and the solid lines represent the Rossin-Rammler fits.

Figure 3 The drift sampling positions and trees used for the field trials

Figure 4 The dimensions of the computational domain and the boundary conditions used in the CFD model. Wind is in the same direction as the direction of spraying.

Figure 5 Wind rose plot showing the magnitude and direction of wind registered at 10m height when a field trial was conducted on an apple classical training system using the cross-flow sprayer fitted with three nozzle arrangements: (a) ATR, (b) TVI and (c) ATR+TVI

Figure 6 Validation of the drift curves predicted by the CFD model for three different nozzle arrangements fitted to a cross-flow sprayer: (a) ATR, (b) TVI (c) ATR+TVI. The red lines represent the model predictions and the black lines represent the measurements (Error bars denote standard deviation). The magnitude and direction of the wind measured at 10m height is shown in Figure 5. Application rate was 500 L ha^{-1} and driving speed was 1.67 m s^{-1}.

Figure 7 Droplet track plots showing the droplet trajectories up to 40 m behind the last tree row for an apple classical training system sprayed with the cross-flow sprayer using three nozzle arrangements: (a) ATR, (b) TVI and (c) ATR+TVI. The tracks are shown on a plane the passes through the middle of the central tree. The track plots are coloured using the diameter of the droplets. Wind velocity was 3 m s^{-1} at 10 m height blowing in the direction of spraying. Application rate was 500 L ha^{-1} and driving speed was 1.67 m s^{-1}.

Figure 8 Contour plots showing the time-integrated spray deposition on the ground for the three nozzle arrangements fitted to a cross-flow sprayer: (a) ATR, (b) TVI and (c) ATR+TVI. Wind velocity was 3 m s^{-1} measured at 10 m height blowing in the direction of spraying. Application rate was 500 L ha^{-1} and driving speed was 1.67 m s^{-1}.

Figure 9 The drift curves predicted by the CFD model for an apple classical training system sprayed with the cross-flow sprayer using three different nozzle arrangements: (a) —— ATR, (b) ······ TVI and (c) – – TVI+ATR. The simulations were done for the same wind velocity of 3 m s^{-1} measured at 10 m height blowing in the direction of spraying. Application rate was 500 L ha^{-1} and driving speed was 1.67 m s^{-1}.

Figure 10 Effect of fan speed on the percentage drift from an apple classical training system sprayed with the cross-flow sprayer using three nozzle arrangements: (a) ATR, (b) TVI and (c) TVI+ATR. The solid and broken lines represent the percentage drift obtained at high and low fan speeds, respectively. The simulations were done for the same wind velocity of 3 m s^{-1} measured at 10 m height blowing in the direction of spraying. Application rate was 500 L ha^{-1} and driving speed was 1.67 m s^{-1}.

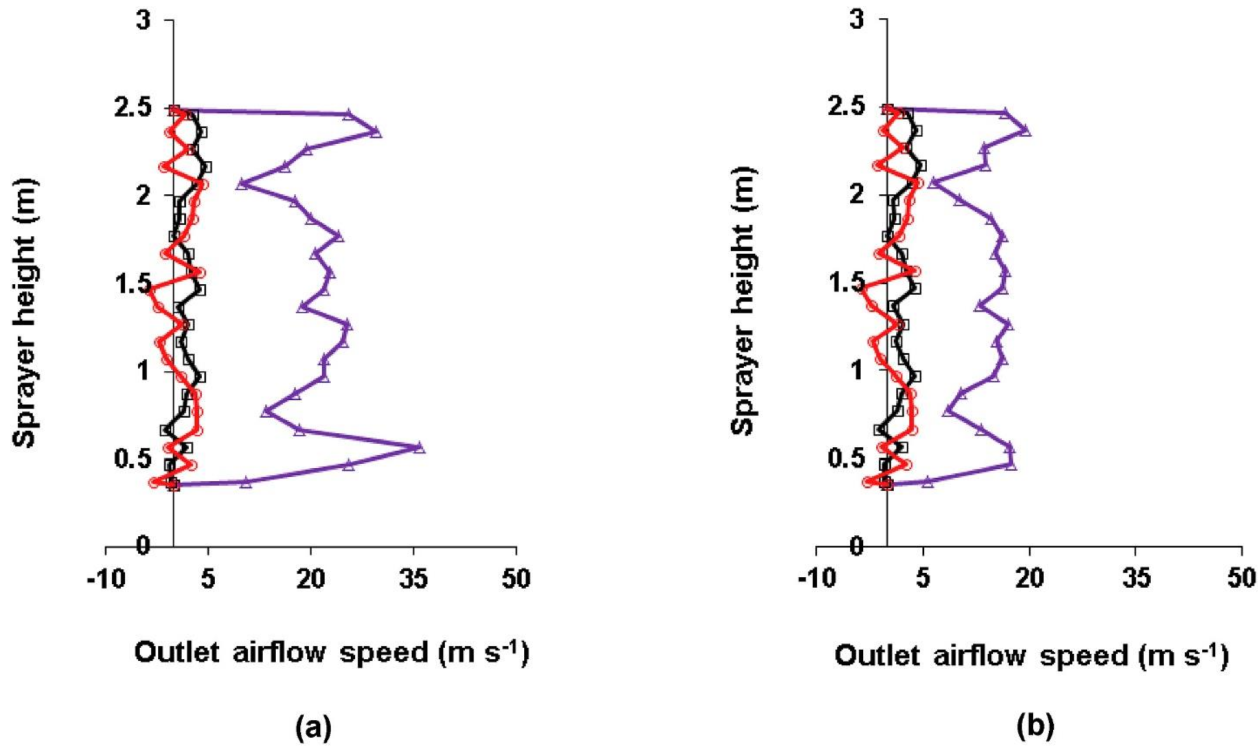

Figure 1 The three components of the outlet velocity of the Cross-flow sprayer (Duoprop, BAB-Bamps, Sint-Truiden, Belgium) used in the analysis operating at high (a) and low fan speeds (b): U (, horizontal perpendicular to driving direction), V (, vertical upward) and W (, horizontal in the driving direction). The outlet velocities were measured at 0.15 m from the outlet area at different heights using 3D ultrasonic sensors (Dekeyser et al., 2013).

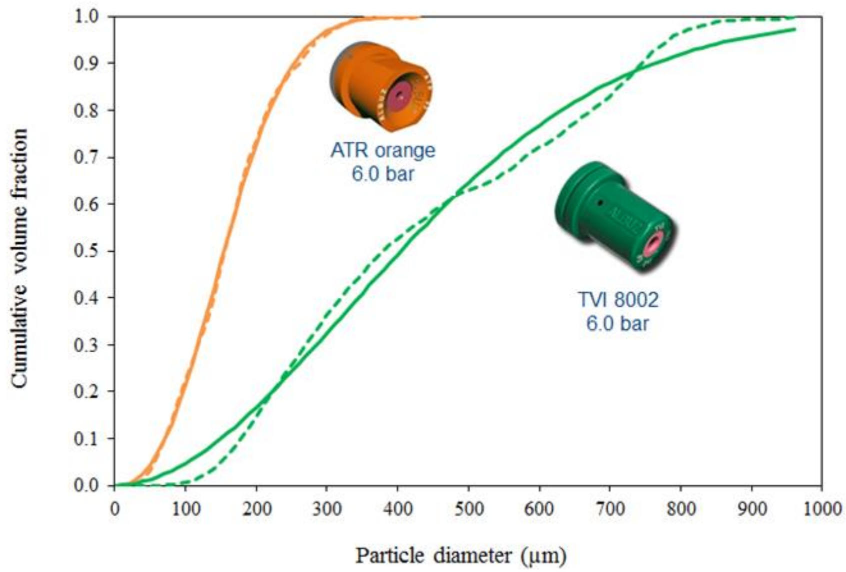

Figure 2 Droplet size distributions and the corresponding Rossin-Rammler fits of two nozzle types. The broken lines represent the measured size distributions and the solid lines represent the Rossin-Rammler fits.

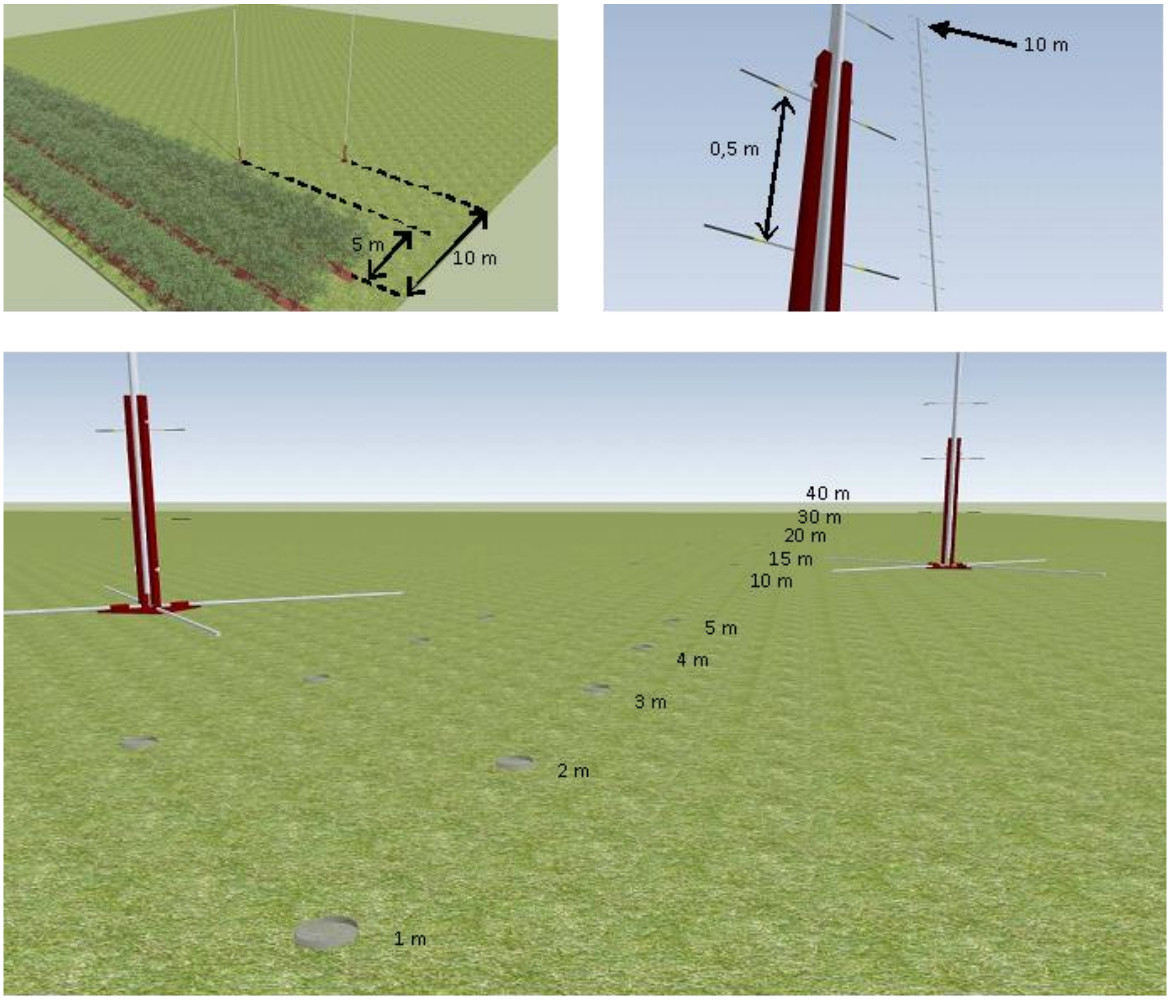

Figure 3 The drift sampling positions and trees used for the field trials

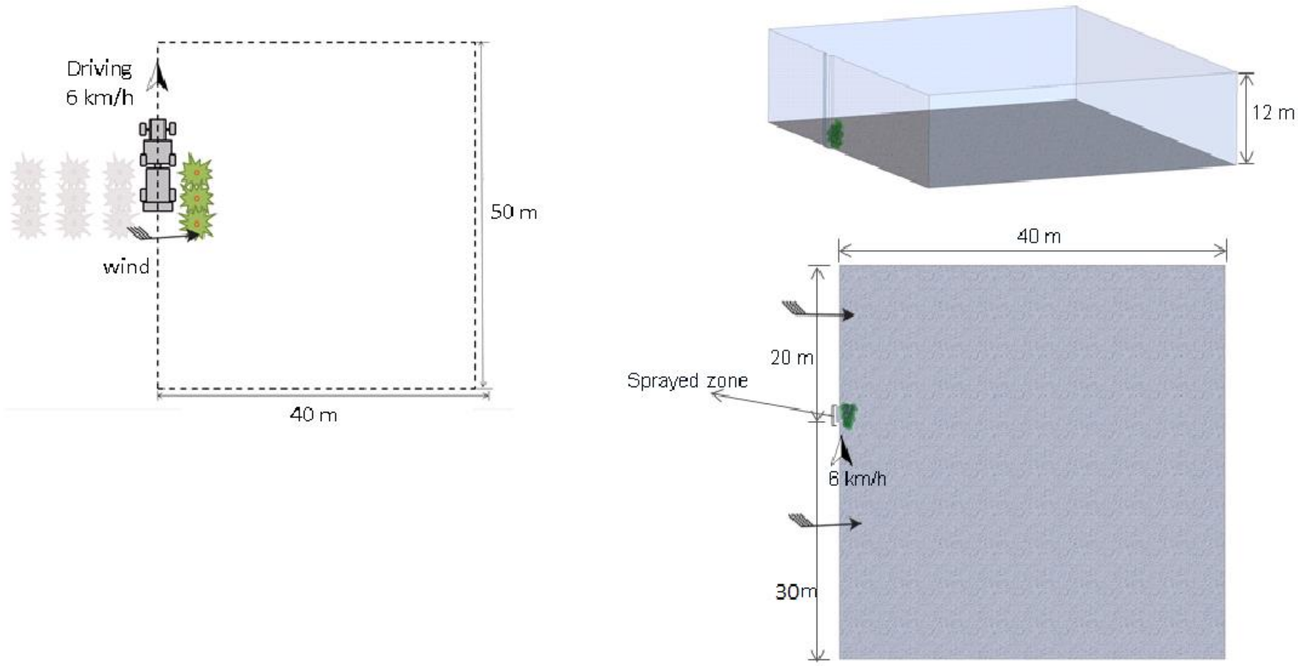

Figure 4 The dimensions of the computational domain and the boundary conditions used in the CFD model. Wind is in the same direction as the direction of spraying.

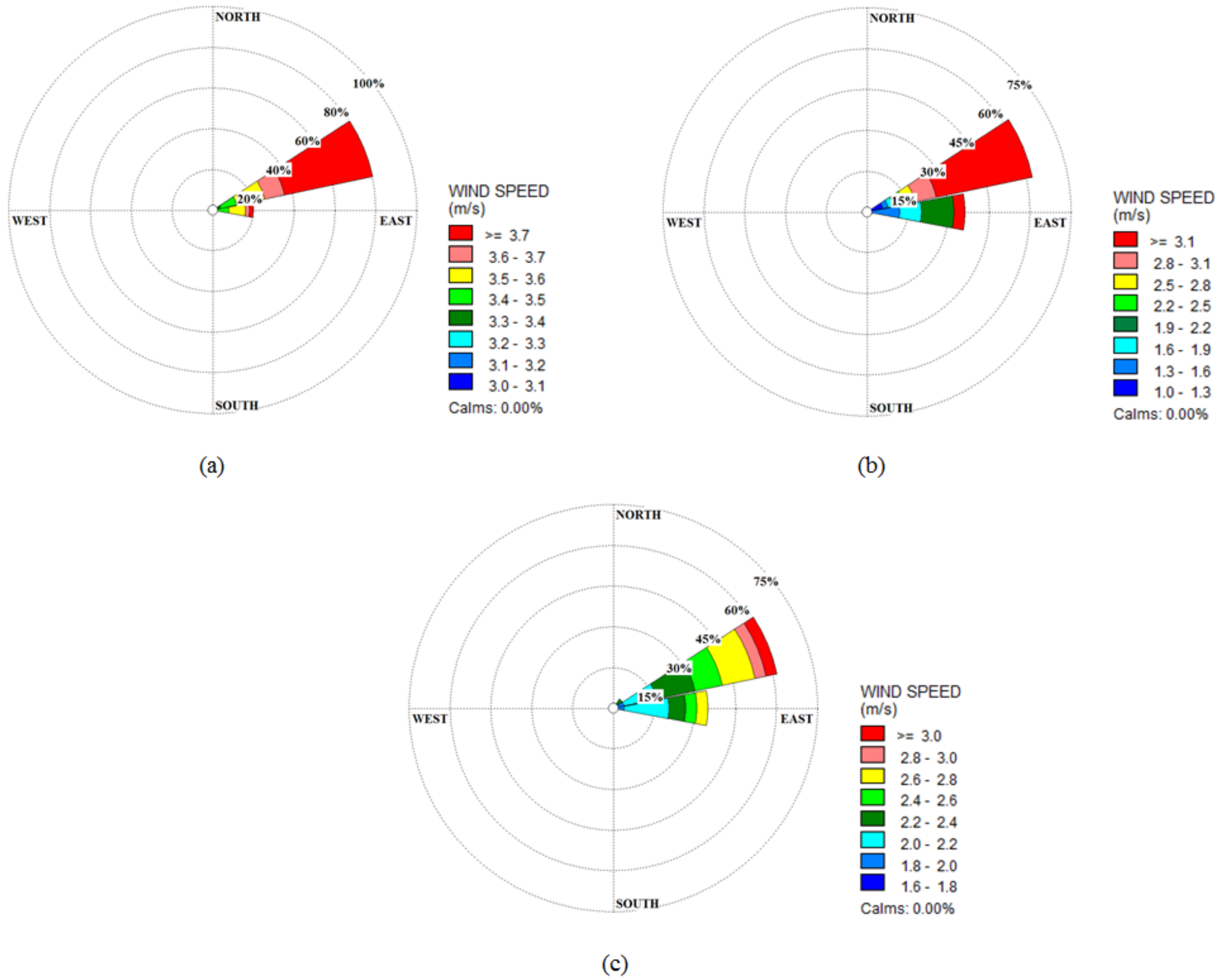

Figure 5 Wind rose plot showing the magnitude and direction of wind registered at 10m height when a field trial was conducted on an apple classical training system using the cross-flow sprayer fitted with three nozzle arrangements: (a) ATR, (b) TVI and (c) ATR+TVI

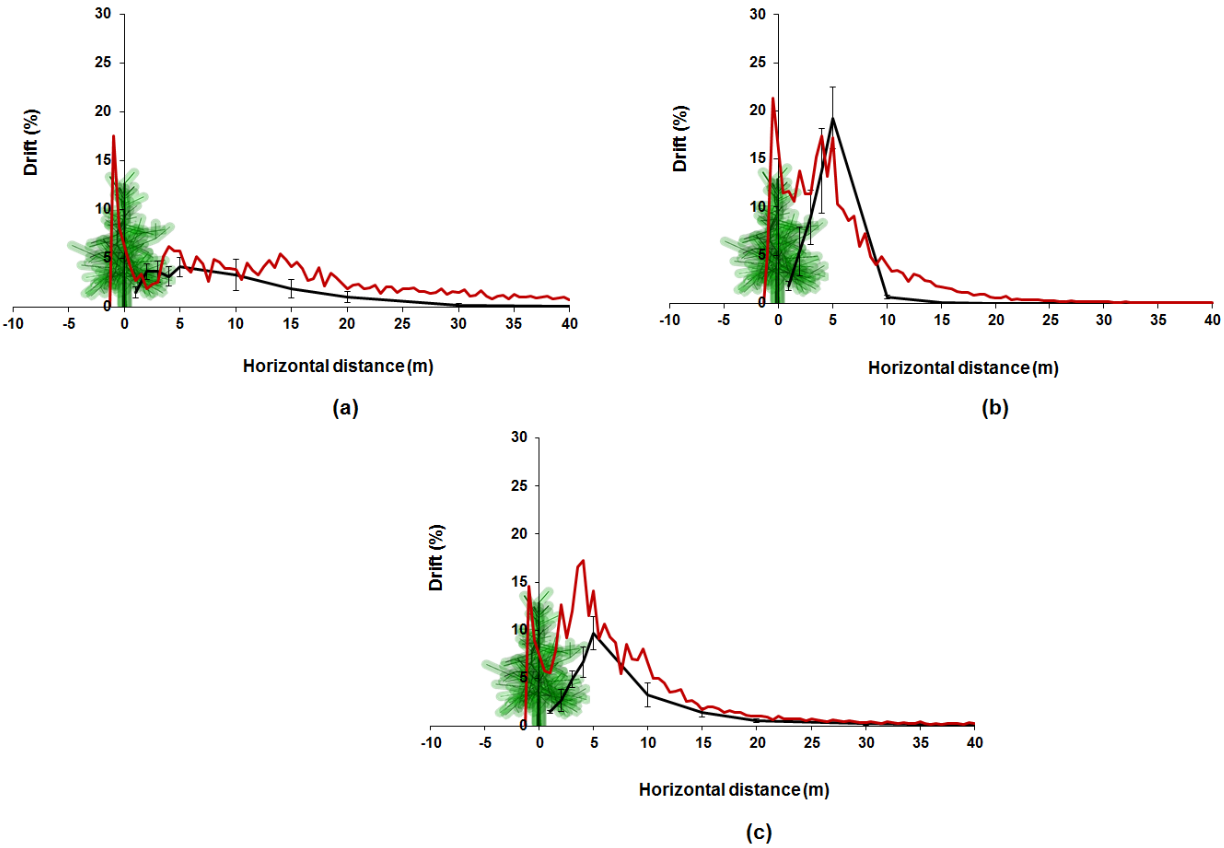

Figure 6 Validation of the drift curves predicted by the CFD model for three different nozzle arrangements fitted to a cross-flow sprayer: (a) ATR, (b) TVI (c) ATR+TVI. The red lines represent the model predictions and the black lines represent the measurements (Error bars denote standard deviation). The magnitude and direction of the wind measured at 10m height is shown in Figure 5. Application rate was 500 L ha^{-1} and driving speed was 1.67 m s^{-1}.

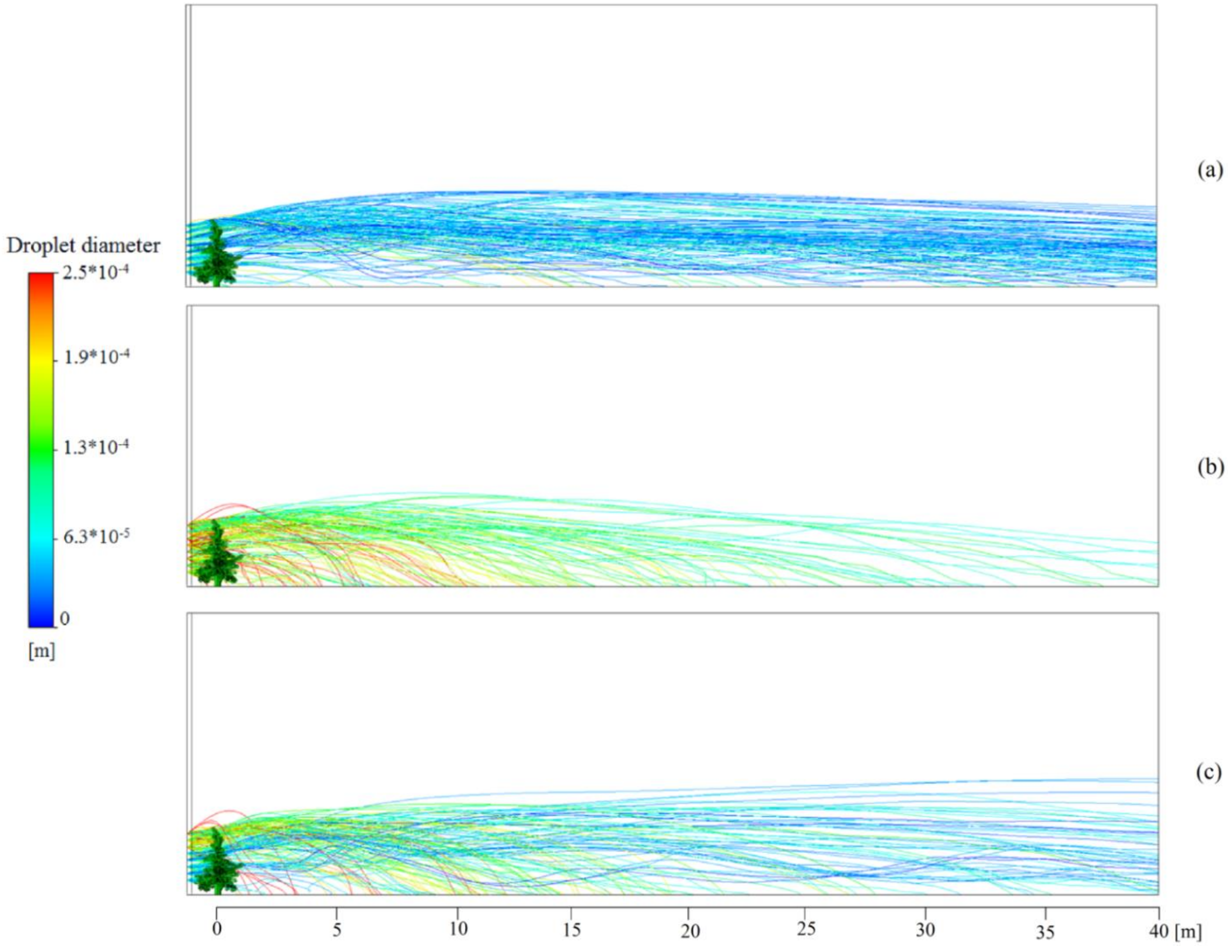

Figure 7 Droplet track plots showing the droplet trajectories up to 40 m behind the last tree row for an apple classical training system sprayed with the cross-flow sprayer using three nozzle arrangements: (a) ATR, (b) TVI and (c) ATR+TVI. The tracks are shown on a plane the passes through the middle of the central tree. The track plots are coloured using the diameter of the droplets. Wind velocity was 3 m s^{-1} at 10 m height blowing in the direction of spraying. Application rate was 500 L ha^{-1} and driving speed was 1.67 m s^{-1}.

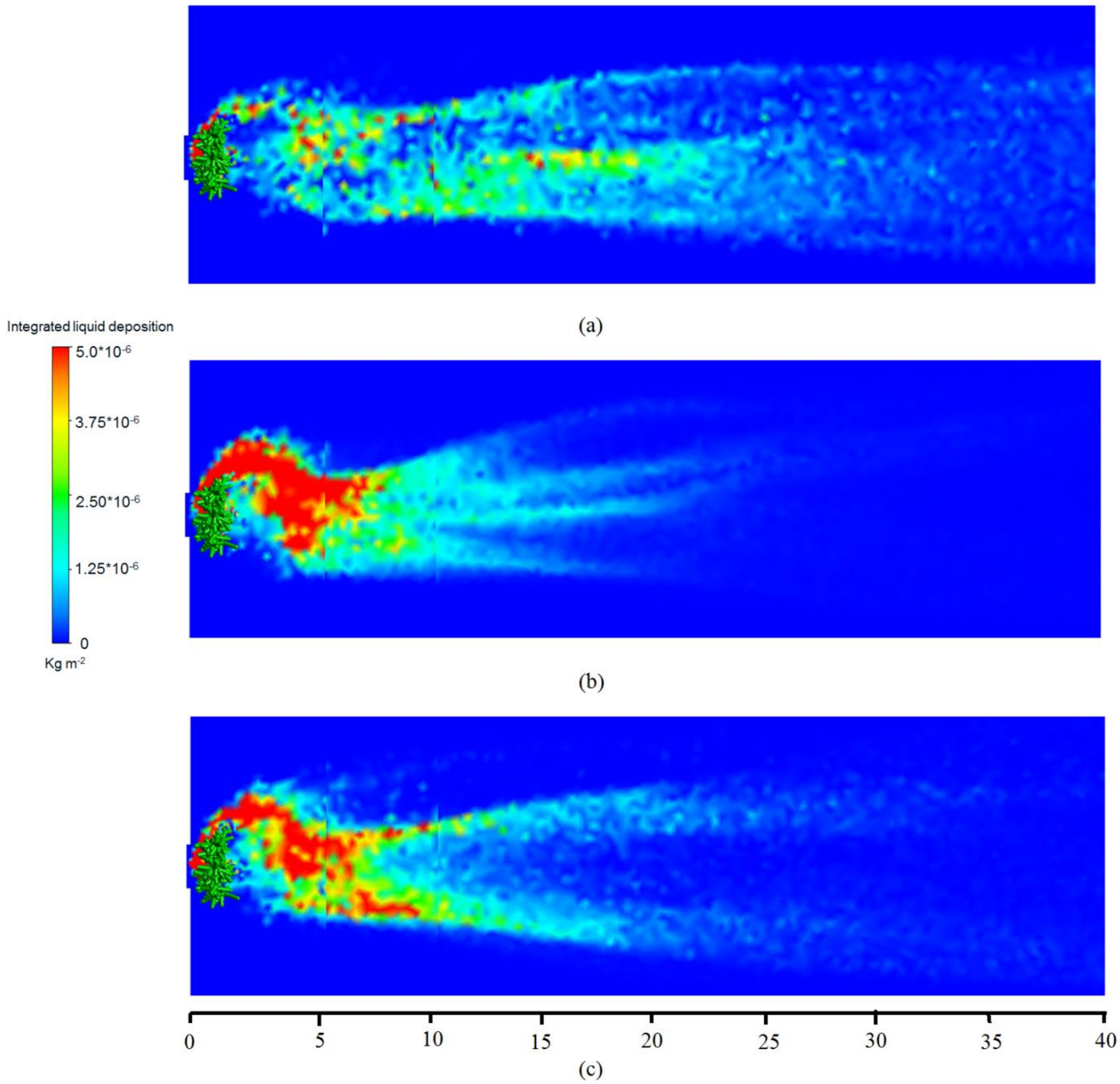

Figure 8 Contour plots showing the time-integrated spray deposition on the ground for the three nozzle arrangements fitted to a cross-flow sprayer: (a) ATR, (b) TVI and (c) ATR+TVI. Wind velocity was 3 m s^{-1} measured at 10 m height blowing in the direction of spraying. Application rate was 500 L ha^{-1} and driving speed was 1.67 m s^{-1}.

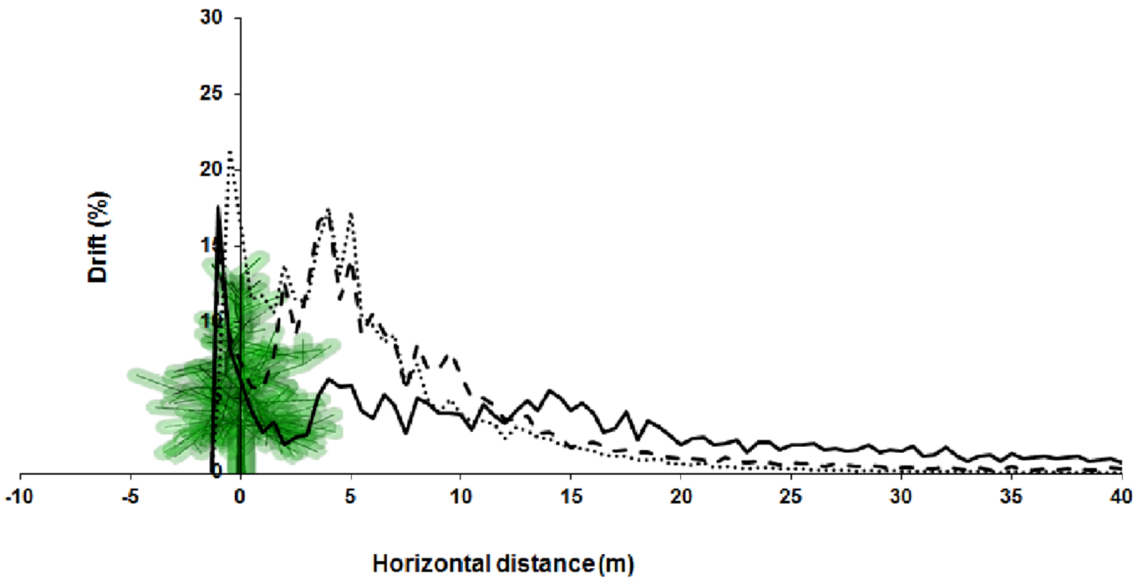

Figure 9 The drift curves predicted by the CFD model for an apple classical training system sprayed with the cross-flow sprayer using three different nozzle arrangements: (a) —— ATR, (b) ⋯⋯ TVI and (c) – – TVI+ATR. The simulations were done for the same wind velocity of 3 m s^{-1} measured at 10 m height blowing in the direction of spraying. Application rate was 500 L ha^{-1} and driving speed was 1.67 m s^{-1}.

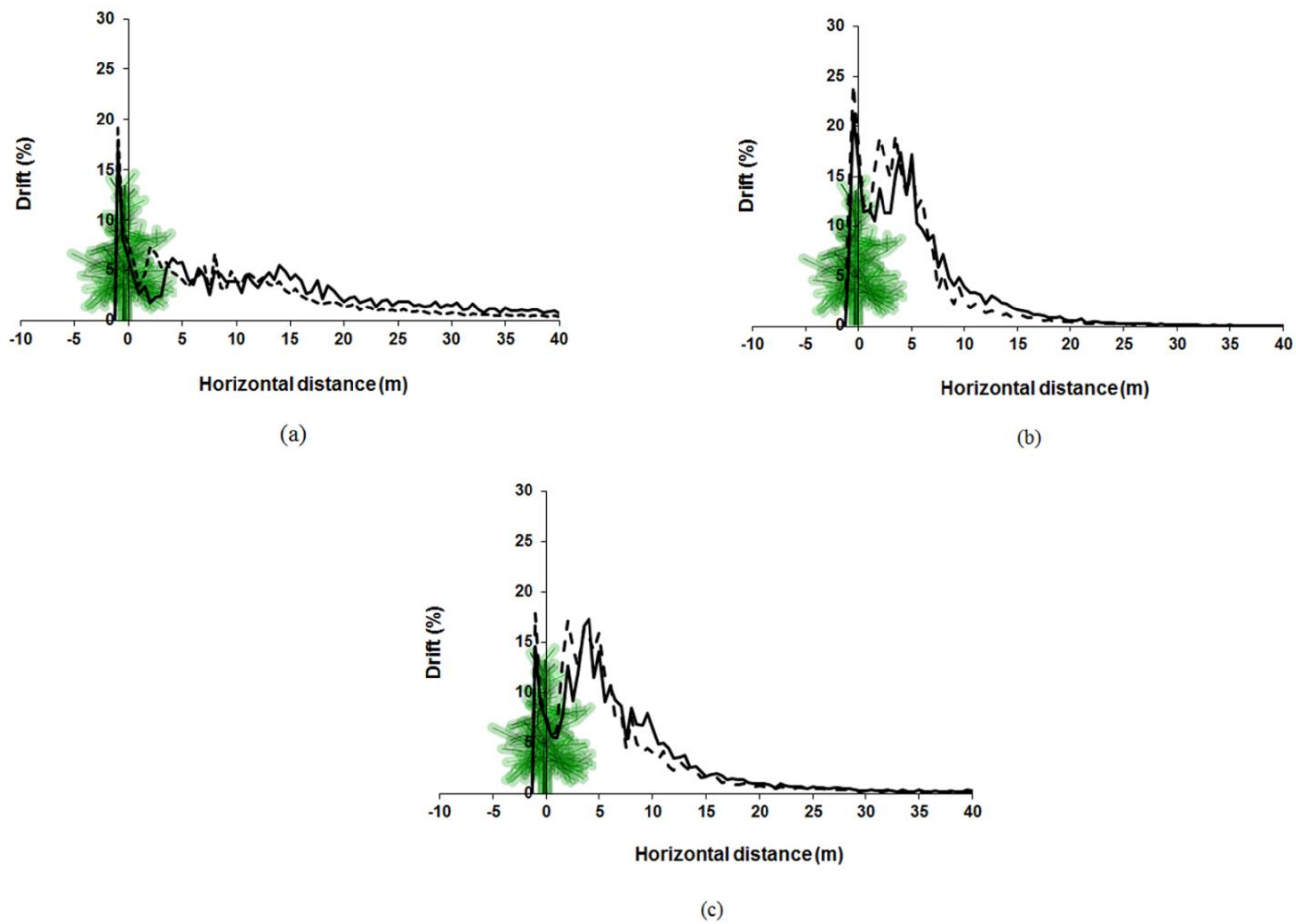

Figure 10 Effect of fan speed on the percentage drift from an apple classical training system sprayed with the cross-flow sprayer using three nozzle arrangements: (a) ATR, (b) TVI and (c) TVI+ATR. The solid and broken lines represent the percentage drift obtained at high and low fan speeds, respectively. The simulations were done for the same wind velocity of 3 m s^{-1} measured at 10 m height blowing in the direction of spraying. Application rate was 500 L ha^{-1} and driving speed was 1.67 m s^{-1}.